

Error-Tolerant Color Rendering for Digital Cameras

Simone Bianco · Raimondo Schettini

Received: 7 May 2013 / Accepted: 10 January 2014 / Published online: 23 January 2014
© Springer Science+Business Media New York 2014

Abstract In digital cameras a color processing pipeline is implemented to convert the RAW image acquired by the camera sensor into a faithful representation of the original scene. There are two main modules in this pipeline: the former is the illuminant estimation and correction module, the latter is the color matrix transformation. In this work we design extended color correction pipelines which exploit the crosstalks between their modules to lead to a higher color rendition accuracy. The effectiveness of the proposed pipelines is shown on a publicly available dataset of RAW images.

Keywords Image processing pipeline · Illuminant estimation · Color correction · Color matrix transformation · Digital camera

1 Introduction

The traditional color correction pipeline for digital cameras is composed by two modules [1–3]: the former is an illuminant estimation and correction module which aims to render the acquired image as close as possible to what a human observer would have perceived if placed in the original scene, emulating the color constancy feature of the human visual system, i.e. the ability of perceiving relatively constant colors when objects are lit by different illuminants

[4–7]. The latter is a color matrix transformation, which is needed for color space transformation as the spectral sensitivity functions of the sensor color channels rarely match those of the desired output color space [8–10].

Although it is known that processing pipelines amplify the noise [11], the color correction modules have been studied and optimized separately, without considering the interactions between them. We have recently shown [12] that the color matrixing stage amplifies the error in the illuminant estimation stage. We have also demonstrated on synthetic data that incorporating knowledge about the illuminant estimation behavior in the optimization of the color correction matrix makes it possible to alleviate this error amplification.

In this work we design and test extended color correction pipelines for digital cameras able to obtain a higher color rendering accuracy. The pipelines proposed in [12] are here further improved in two ways: (i) in the illuminant estimation and correction stage, the traditional diagonal model of illuminant change is replaced by a generalized diagonal transform found by optimization; (ii) the color matrixing stage, usually performed using a linear transformation matrix optimized assuming that the illuminant in the scene has been successfully estimated and compensated for [8–10], is extended exploiting polynomial color space conversions incorporating knowledge about illuminant estimation module behavior.

Experimental results on a standard dataset of raw images show the feasibility of the proposed extended pipelines whatever the illuminant estimation algorithm used here.

2 Image Formation and Color Correction Pipeline

An image acquired by a digital camera can be represented as a function ρ mainly dependent on three physical factors:

S. Bianco (✉) · R. Schettini
Dipartimento di Informatica, Sistemistica e Comunicazione,
Università degli Studi di Milano-Bicocca, Viale Sarca 336,
20126 Milano, Italy
e-mail: bianco@disco.unimib.it

R. Schettini
e-mail: schettini@disco.unimib.it

the illuminant spectral power distribution $I(\lambda)$, the surface spectral reflectance $S(\lambda)$, and the sensor spectral sensitivities $\mathbf{C}(\lambda)$. Using this notation, the sensor responses at the pixel with coordinates (x, y) can be thus described as:

$$\rho(x, y) = \int_{\omega} I(x, y, \lambda) S(x, y, \lambda) \mathbf{C}(\lambda) d\lambda, \quad (1)$$

where ω is the wavelength range of the visible light spectrum, ρ and $\mathbf{C}(\lambda)$ are three-component vectors. Since the three sensor spectral sensitivities are usually more sensitive respectively to the low, medium and high wavelengths, the three-component vector of sensor responses $\rho = (\rho_1, \rho_2, \rho_3)$ is also referred to as the sensor or camera raw $\mathbf{RGB} = (R, G, B)$ triplet. In the following we adopt the convention that \mathbf{RGB} triplets are represented by column vectors.

In order to render the acquired image as close as possible to what a human observer would have perceived if placed in the original scene, the first stage of the color correction pipeline aims to emulate the color constancy feature of the human visual system (HVS), i.e. the ability to perceive relatively constant colors when objects are lit by different illuminants. The dedicated module is usually referred to as automatic white balance (AWB), which aims to determine from the image content the color of the ambient light and compensate for its effects. Numerous methods exist in the literature and Hordley [4], Ebner [5], Foster [6], and Gijzen et al. [7] give excellent reviews of them. Most of them are based on the simplifying assumption that the illuminant in the scene is uniform, with a few exceptions [41–45]. In the following we assume uniform illuminant. Once the color of the ambient light has been estimated, in general its compensation is based on an independent regulation of the three color signals through three different gain coefficients [13, 33]. This correction can be easily implemented on digital devices as a diagonal matrix multiplication. The application of non-diagonal illuminant compensation matrices could further improve the results, but only in case of broad sensor spectral sensitivities [40].

The second stage of the color correction pipeline transforms the image data into a standard RGB color space (e.g. sRGB, ITU-R BT.709). This transformation, usually called color matrixing, is needed because the spectral sensitivity functions of the sensor color channels rarely match those of the desired output color space. Typically this transformation is a 3-by-3 matrix with 9 variables to be determined. There are both algebraic [8, 9] and optimization-based methods [10] to find them.

The traditional color correction pipeline [1–3], which assumes a uniform illuminant across the scene, can be de-

Table 1 Notation adopted

Symbol	Description
$\mathbb{1}_3$	3×3 identity matrix
$\mathbb{0}_{3,t-3}$	zero matrix with size $3 \times (t - 3)$
t	number of terms of the transformation \mathcal{T} used
m	number of different matrices to use in the MILLWEB strategy
s	number of images used in the optimization
\mathbf{u}	weight distribution (assumed uniform in the experiments)
n	number of colored patches of the color target used
\mathbf{r}_k	color coordinates of the k -th patch in the chosen standard color space
\mathbf{c}_k	color coordinates of the k -th patch in the camera color space
\mathcal{E}	chosen error metric
\mathbf{G}_j	diagonal illuminant correction matrix for the j -th image
\mathcal{T}	polynomial transformation chosen to be applied to the illuminant-compensated RGB values
α	exposure correction gain

scribed as follows:

$$\begin{bmatrix} R \\ G \\ B \end{bmatrix}_{out} = \left(\alpha \begin{bmatrix} a_{11} & a_{12} & a_{13} \\ a_{21} & a_{22} & a_{23} \\ a_{31} & a_{32} & a_{33} \end{bmatrix} \times \begin{bmatrix} r_{awb} & 0 & 0 \\ 0 & g_{awb} & 0 \\ 0 & 0 & b_{awb} \end{bmatrix} \begin{bmatrix} R \\ G \\ B \end{bmatrix}_{in} \right)^{\gamma} \quad (2)$$

where \mathbf{RGB}_{in} are the camera raw \mathbf{RGB} values, α is an exposure compensation common gain, the diagonal matrix $\text{diag}(r_{awb}, g_{awb}, b_{awb})$ is the channel-independent gain compensation of the illuminant, the full 3-by-3 matrix $a_{(i,j)}$, $(i, j) = \{1, 2, 3\}^2$ is the color space conversion transform from the device-dependent RGB to the sRGB color space, γ is the gamma correction defined for the sRGB color space and \mathbf{RGB}_{out} are the output sRGB values.

3 Pipeline Extension

In this section we describe how the traditional pipeline and the pipelines originally proposed in [12] can be extended in order to obtain an higher color accuracy. In the following a more compact version of Eq. (2) is used:

$$\mathbf{RGB}_{out} = (\alpha \mathbf{A} \mathbf{I}_w \cdot \mathbf{RGB}_{in})^{\gamma} \quad (3)$$

where α , \mathbf{I}_w and \mathbf{A} respectively represent the exposure compensation gain, the diagonal matrix for the illuminant compensation and the color matrix transformation. The notation adopted is reported in Table 1.

The pipeline in Eq. (3) exploits a diagonal model of illuminant change. However, it is known that this model does not perform properly in the case the camera sensors are broad functions [33], which is usually the case. We try to convert the camera sensors into a set of more narrow ones, for which the diagonal model holds. This approach falls under the name of sensor sharpening and the resulting transform is usually referred to as generalized diagonal transform (GDT) [33]. The pipeline in Eq. (3) can be thus extended in:

$$\mathbf{RGB}_{out} = (\alpha \mathbf{A}(\mathbf{C}^{-1} \mathbf{I}_w \mathbf{C}) \cdot \mathbf{RGB}_{in})^\gamma \tag{4}$$

where \mathbf{C} is the sensor sharpening transform, and $\mathbf{C}^{-1} \mathbf{I}_w \mathbf{C}$ is the generalized diagonal transform.

Sensor sharpening is a common strategy when the source and destination illuminants are perfectly known [35, 36]. We propose here an operative method, based on optimization, to find a generalized diagonal transform able to deal with the case that the scene illuminant, that has to be estimated, is affected of error.

In the pipelines of Eqs. (3) and (4) the color space conversion is implemented by a 3×3 matrix (\mathbf{A}), which works on the linear sensor values. The pipeline is here extended to incorporate polynomial color space conversions (and thus rectangular matrices \mathbf{A}) by defining a transformation \mathcal{T} which defines the polynomial transformation to be applied to the illuminant-compensated RGB values:

$$\mathbf{RGB}_{out} = (\alpha \mathbf{A} \mathcal{T}((\mathbf{C}^{-1} \mathbf{I}_w \mathbf{C}) \cdot \mathbf{RGB}_{in}))^\gamma \tag{5}$$

Although polynomial color conversion is a common approach for the characterization of digital scanners [30] and fixed camera/light setups [26, 37], it is unknown if it can be effectively applied in the color correction pipeline of a digital camera as it is also unknown how polynomial color corrections amplify the error in the illuminant estimation compared with linear color correction.

In this work three different kinds of transformation \mathcal{T} have been used. The first one is the identity, so that the color correction is done with linear polynomial:

$$\mathcal{T}_1([R \ G \ B]) = [R \ G \ B] \tag{6}$$

The second one is the rooted polynomial (second degree) [29]:

$$\mathcal{T}_{2R}([R \ G \ B]) = [R \ G \ B \ \sqrt{RG} \ \sqrt{RB} \ \sqrt{GB}] \tag{7}$$

The third one is the second order polynomial [32]:

$$\mathcal{T}_2([R \ G \ B]) = [R \ G \ B \ R^2 \ G^2 \ B^2 \ RG \ RB \ GB] \tag{8}$$

3.1 Single Illuminant Color Correction Pipeline

Given a transformation \mathcal{T} , the first color correction pipeline considered is named Single ILLuminant (SILL) since it is

based on a single matrix transform optimized for a single illuminant. Given a set of n different patches whose sRGB values \mathbf{r} are known, and the corresponding camera raw values \mathbf{c} measured by the sensor when the patches are lit by the chosen illuminant, we want to find the optimal matrices $[\mathbf{A}, \mathbf{C}]$ and the optimal exposure value α , which we respectively call $[\hat{\mathbf{A}}, \hat{\mathbf{C}}, \hat{\alpha}]$, that satisfy:

$$[\hat{\mathbf{A}}, \hat{\mathbf{C}}, \hat{\alpha}] = \underset{\substack{\mathbf{A} \in \mathbb{R}^{3 \times t} \\ \mathbf{C} \in \mathbb{R}^{3 \times 3}}}{\operatorname{argmin}} \sum_{k=1}^n \mathcal{E}(\mathbf{r}_k, (\alpha \mathbf{A} \mathcal{T}(\mathbf{C}^{-1} \mathbf{I}_w \mathbf{C}) \mathbf{c}_k)^\gamma) \tag{9}$$

where \mathcal{E} is the chosen error metric, and the subscript k indicates the triplet in the k th column of the matrix, i.e. it indicates the trichromatic values of the k th patch. The error metric \mathcal{E} adopted is the average ΔE_{94} colorimetric error between the reference and calculated sRGB values mapped in the CIELab color space. The ΔE_{94} metric has been chosen because of its perceptual uniformity in color imaging [1]. Given the importance of neutrals in the color reproduction, the $3t$ degrees of freedom of the color matrix transformation are usually reduced to $3(t - 1)$ by a white point preserving constraint, i.e. a neutral color in the device dependent color space should be mapped to a neutral color in the device independent color space. This can be easily obtained by constraining each row to sum to one.

3.2 Single Illuminant Color Correction Pipeline with White Balance Error Buffer

The second color correction pipeline considered is named Single ILLuminant with White balance Error Buffer (SILLWEB). It is based on a single matrix transform optimized for a single illuminant, taking into account the behavior of the AWB module used. Suppose that the ground truth gain coefficients $\mathbf{g}_0 = [r_0, g_0, b_0]$ have been already determined and reshaped in the diagonal transform G_0 to compensate the considered illuminant; we generate a set $\mathbf{g} = \{\mathbf{g}_1, \dots, \mathbf{g}_s\}$ of s gain coefficients with different distances along different hue directions from \mathbf{g}_0 , measured using the angular distance. These can be used to simulate errors that may occur in the AWB process and are paired with a weights distribution $\mathbf{u} = \{u_0, \dots, u_s\}$ reflecting the frequency of the considered errors. The ground truth gains \mathbf{g}_0 are computed from the camera raw values measured by the sensor when a neutral patch is lit by the chosen illuminant. The sets \mathbf{g} and \mathbf{u} could be derived in two different ways:

- \mathbf{g} could be generated by sampling uniformly the hue circle and for each sampled hue direction the desired gains with given angular distances from \mathbf{g}_0 could be obtained by brute force search; \mathbf{u} can be then estimated from a set of synthetic images generated according to Eq. (1).
- \mathbf{g} could be directly obtained from a dataset of natural RAW images, thus obtaining an entry g_j for each image in the dataset; in this case \mathbf{u} can be set uniform.

Algorithm 1 SILL-WEB($\mathbf{r}, \mathbf{G}, \mathbf{c}$)

```

 $\mathbf{A} \leftarrow [\mathbb{1}_3 \ \mathbf{0}_{3,t-3}]$ 
 $\mathbf{C} \leftarrow \mathbb{1}_3$ 
 $\boldsymbol{\alpha} = [\alpha_0, \dots, \alpha_s] \leftarrow [1, \dots, 1]$ 
initialize  $\mathbf{u}$ 
repeat
    find  $\hat{\mathbf{A}}, \hat{\mathbf{C}}$  s.t. Eq. (10) is satisfied
     $\mathbf{A} \leftarrow \hat{\mathbf{A}}$ 
     $\mathbf{C} \leftarrow \hat{\mathbf{C}}$ 
    for image number  $j = 1$  to  $s$ 
        find  $\alpha$  s.t.
         $\operatorname{argmin}_{\alpha} \sum_{k=1}^n \mathcal{E}(\mathbf{r}_k, (\alpha \mathbf{A} \mathcal{T}(\mathbf{C}^{-1} \mathbf{G}_j \mathbf{C}) \mathbf{c}_k)^\gamma)$ 
         $\alpha_j \leftarrow \alpha$ 
until convergence or stopping criteria are met
return  $(\mathbf{A}, \mathbf{C}, \boldsymbol{\alpha})$ 
    
```

In this work we have used the second approach for all the color correction pipelines proposed. The optimization problem can be thus formulated as:

$$\begin{aligned}
 & [\hat{\mathbf{A}}, \hat{\mathbf{C}}, \hat{\boldsymbol{\alpha}}] \\
 & = \operatorname{argmin}_{\substack{\mathbf{A} \in \mathbb{R}^{3 \times t} \\ \mathbf{C} \in \mathbb{R}^{3 \times 3} \\ \alpha_j \in \mathbb{R}}} \sum_{j=0}^s u_j \left(\sum_{k=1}^n \mathcal{E}(\mathbf{r}_k, (\alpha_j \mathbf{A} \mathcal{T}(\mathbf{C}^{-1} \mathbf{G}_j \mathbf{C}) \mathbf{c}_k)^\gamma) \right)
 \end{aligned} \tag{10}$$

$$\text{subject to } \sum_{j=1}^t A_{(i,j)} = 1, \quad \forall i \in \{1, 2, 3\}$$

where $\mathbf{G}_j, j = \{0, \dots, s\}$ are the diagonal matrices obtained respectively by reshaping the gain coefficients $\{\mathbf{g}_0, \dots, \mathbf{g}_s\}$. The pseudo-code for the SILL-WEB color correction strategy is reported in Algorithm 1.

3.3 Multiple Illuminant Color Correction Pipeline with White Balance Error Buffer

The third color correction pipeline considered is named Multiple ILLuminant with White balance Error Buffer (MILL-WEB). It differs from the previous pipeline since it is based on multiple matrix transforms, with each one optimized for a different taking illuminant. For each image different matrix transforms \mathbf{A} and \mathbf{C} are therefore used: when the AWB algorithm is applied to estimate the illuminant compensation gains $\hat{\mathbf{g}}$, the two chosen taking illuminants ILL_i and ILL_j with the most similar gains $\mathbf{g}_{0,i}$ and $\mathbf{g}_{0,j}$ are identified, and the matrix transforms are calculated as follows:

$$\mathbf{A} = \tau \mathbf{A}_{\text{ILL}_i} + (1 - \tau) \mathbf{A}_{\text{ILL}_j} \tag{11}$$

Algorithm 2 MILL-WEB($\mathbf{r}, \mathbf{G}, \mathbf{c}, m$)

```

cluster  $\mathbf{G}$  to find  $m$  centroids
for  $i = 1$  to  $m$ 
     $\mathbf{A}_i \leftarrow [\mathbb{1}_3 \ \mathbf{0}_{3,t-3}]$ 
     $\mathbf{C}_i \leftarrow \mathbb{1}_3$ 
    initialize  $\mathbf{u}_i$ 
 $\boldsymbol{\alpha} = [\alpha_0, \dots, \alpha_s] \leftarrow [1, \dots, 1]$ 
repeat
    for  $i = 1$  to  $m$ 
        find  $z_1, \dots, z_h$  s.t.  $\forall z_i : \mathbf{G}_{z_i} \in \text{centroid } C_i$ 
         $\mathbf{u} \leftarrow \mathbf{u}_i$ 
        find  $\hat{\mathbf{A}}, \hat{\mathbf{C}}$  s.t. Eq. (10) is satisfied
         $\mathbf{A}_i \leftarrow \hat{\mathbf{A}}$ 
         $\mathbf{C}_i \leftarrow \hat{\mathbf{C}}$ 
        for image number  $j = z_1$  to  $z_h$ 
            compute  $\mathbf{A}$  and  $\mathbf{C}$  using Eqs. (11) and (12)
            find  $\alpha$  s.t.
             $\operatorname{argmin}_{\alpha} \sum_{k=1}^n \mathcal{E}(\mathbf{r}_k, (\alpha \mathbf{A} \mathcal{T}(\mathbf{C}^{-1} \mathbf{G}_{z_j} \mathbf{C}) \mathbf{c}_k)^\gamma)$ 
             $\alpha_{z_j} \leftarrow \alpha$ 
until convergence or stopping criteria are met
return  $([\mathbf{A}_1, \dots, \mathbf{A}_m], [\mathbf{C}_1, \dots, \mathbf{C}_m], \boldsymbol{\alpha})$ 
    
```

$$\mathbf{C} = \tau \mathbf{C}_{\text{ILL}_i} + (1 - \tau) \mathbf{C}_{\text{ILL}_j} \tag{12}$$

where

$$\tau = \frac{D(\hat{\mathbf{g}}, \mathbf{g}_{0,j})}{D(\hat{\mathbf{g}}, \mathbf{g}_{0,i}) + D(\hat{\mathbf{g}}, \mathbf{g}_{0,j})} \tag{13}$$

and D is the angular error between the gains considered, i.e.

$$D(\mathbf{g}_1, \mathbf{g}_2) = \arccos \left(\frac{\mathbf{g}_1^T \cdot \mathbf{g}_2}{\|\mathbf{g}_1\| \cdot \|\mathbf{g}_2\|} \right) \tag{14}$$

The pseudo-code for the MILL-WEB color correction strategy is reported in Algorithm 2. Instead of deciding arbitrarily the m taking illuminants for which derive the matrix transforms, the first step of the MILL-WEB pseudo-code consists in the clustering of the ground-truth gains of the images in the dataset of natural RAW images used. Since they are 3×3 diagonal matrices, this is achieved by applying the k -means algorithm [25] to the diagonal of the matrices by treating them as points in the \mathbb{R}^3 space.

4 Experimental Results

The aim of the designed experiments is to verify if the proposed extended pipelines improve the color accuracy over

the traditional pipeline and the strategies proposed in [12], whatever the AWB algorithm adopted.

In our previous work [12], we used a digital camera simulator for all the experiments. Here, to test the performance of the investigated processing pipelines, a standard dataset of RAW camera images having a known color target is used [23, 28]. This dataset is captured using two high-quality digital SLR cameras in RAW format (Canon 1D and Canon 5D), and is therefore free of any color correction. The dataset consists of a total of 568 images, both indoor (246) and outdoor (322). The Canon 1D was used to acquire 86 images, the Canon 5D to acquire the remaining 482 images. The Macbeth ColorChecker (MCC) chart is included in every scene acquired, and this allows to accurately estimate the scene illuminant. The MCC is composed by a total of 24 patches, 6 of which form a gray scale from white to black. The ground truth gains \mathbf{g}_0 for each image are obtained from the RAW values recorded by the sensor for the gray scale: let us call $\mathbf{RGB}_{g_1}, \dots, \mathbf{RGB}_{g_6}$ the average \mathbf{RGB} values for the central region of each acquired gray patch; \mathbf{g}_0 is then computed as follows:

$$\mathbf{g}_0 = \left(\text{median} \begin{bmatrix} \mathbf{RGB}_{g_1} / \|\mathbf{RGB}_{g_1}\|_\infty \\ \mathbf{RGB}_{g_2} / \|\mathbf{RGB}_{g_2}\|_\infty \\ \vdots \\ \mathbf{RGB}_{g_6} / \|\mathbf{RGB}_{g_6}\|_\infty \end{bmatrix} \right)^{-1} \quad (15)$$

where both the computation of the median value and the inverse are meant component-wise.

In the last years several algorithms have been proposed with the aim of improving the accuracy of illuminant estimation. A comparison of these algorithms is given for example in [7, 34]. The automatic white balance modules considered have been chosen to be representative of the state of the art and range from low-level statistics based [17], gamut mapping based [14, 16, 27], and classification based [15, 22].

The first one is the ideal illuminant estimator, which uses the ground truth illuminant for each scene.

The next four algorithms correspond to different instances of the general equation derived in [17]:

$$\mathbf{I}(d, p, \sigma) = \frac{1}{k} \left(\iint |\nabla^d \rho_\sigma(x, y)|^p dx dy \right)^{\frac{1}{p}}, \quad (16)$$

and correspond to the Gray World (GW) [18], White Patch (WP) [19], Shades of Gray (SOG) [20], and General Gray World (GGW) [17]. The parameter d is the order of the spatial derivative, p is the Minkowski norm, $\rho_\sigma(x, y) = \rho(x, y) \otimes G_\sigma(x, y)$ is the convolution of the image with a Gaussian filter $G_\sigma(x, y)$ with scale parameter σ , and k is a constant to be chosen such that the illuminant color \mathbf{I} has unit length (using the 2-norm). The parameters (d, p, σ) for the algorithms considered are set as in [7].

Table 2 AWB performance: median angular errors between estimated and ground truth illuminants for the whole image dataset, and for each camera separately

Algorithm	Whole DB	Canon 1D	Canon 5D
ID	0.0°	0.0°	0.0°
GW	6.3°	4.7°	6.6°
WP	7.5°	8.4°	7.3°
SOG	4.9°	4.9°	4.8°
GGW	4.6°	4.8°	4.6°
GM	4.1°	5.2°	3.9°
FB	2.9°	4.0°	2.8°

The sixth algorithm considered is the Gamut Mapping (GM), which assumes that for a given illuminant, one observes only a limited gamut of colors [27]. It has a training phase in which a canonical illuminant is chosen and the canonical gamut is computed observing as many surfaces under the canonical illuminant as possible. Given an input image with an unknown illuminant, its gamut is computed and the illuminant is estimated as the mapping that can be applied to the gamut of the input image, resulting in a gamut that lies completely within the canonical gamut and produces the most colorful scene.

The seventh algorithm considered is the Feature Based (FB) algorithm described in [22]. It is based on five independent AWB algorithms [21] and a classification step which automatically selects, which AWB algorithm to use for each image. The classifier is trained on low level features automatically extracted from the images.

The AWB performance are measured with the angular error between the estimated and the ground truth illuminant. The median angular error for each investigated algorithm on the whole image dataset, and for each camera separately, are reported in Table 2. It is possible to note that no algorithm is error free, and that the more complex ones outperform those based on low-level statistics.

The evaluation procedure adopted for a generic color correction pipeline is the following: each AWB algorithm is applied to the image under consideration, excluding the MCC chart region. For each algorithm estimation, the color correction pipelines described in Sect. 3 are then applied to the whole image. For each color corrected image, the MCC chart is extracted [31] and the average sRGB values of the central area of each patch are calculated and mapped in CIELab using standard equations [12]. The color accuracy of the pipeline under consideration is measured in terms of the average ΔE_{94} error between the CIELab color coordinates of the color corrected MCC patches and their theoretical CIELab values given in [24].

For the single illuminant color correction pipelines (SILL), the taking illuminant is chosen to be the one in the

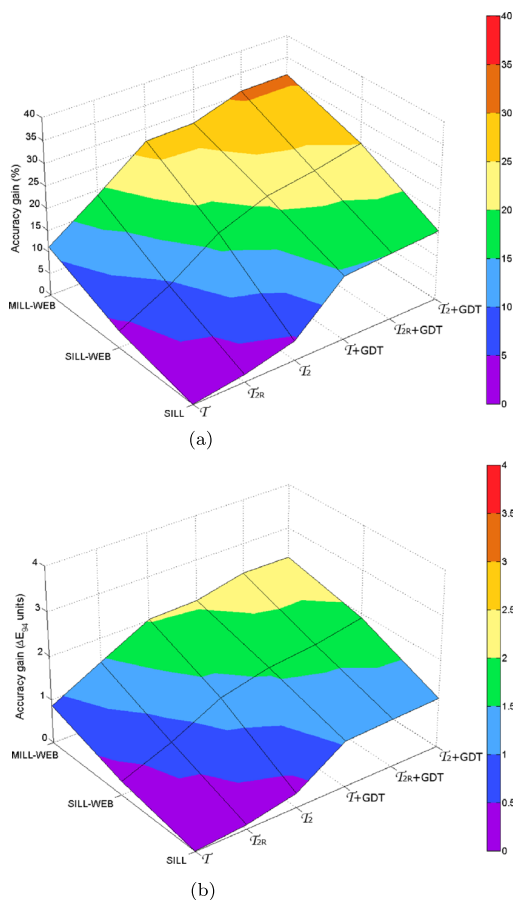


Fig. 1 Average percentage (a) and absolute (b) improvement of the colorimetric error by the different extended pipelines on the whole image dataset

image with the lowest angular distance from the camera daylight multipliers. For the single and multiple illuminant color correction pipelines with white balance error buffer (SILL-WEB and MILL-WEB), the matrices and taking illuminants are computed exploiting the whole dataset using a leave-one-out cross validation scheme: at turn each image is left out and the rest of the images taken with the same camera are used for the optimization. For the multiple illuminant color correction pipeline (MILL-WEB) the number of taking illuminants is set to $m = 7$ as in [12]. For all the color correction pipelines compared, the best matrices satisfying Eqs. (9) and (10) are found by optimization using as c_k all the 24 patches of the MCC. The Pattern Search Method (PSM) is here used as optimization algorithm. PSMs are a class of direct search methods for nonlinear optimization [38, 39] that do not require any explicit estimate of derivatives. The termination condition used is the one that occurred first between the convergence criteria and the stopping criteria. The former consists in a reduction of the current best solution below $1 \cdot 10^{-14}$, the latter in the reaching of the maximum number of iterations set to $1 \cdot 10^4$.

In Fig. 1, taking the traditional pipeline (SILL strategy with the 3×3 color correction matrix) as baseline, the average percentage and absolute improvements of the color accuracy of the different pipelines are reported. They are averaged over all the images composing the dataset, and the different AWB algorithms considered. The marks on the left-hand side axis are relative to the different color correction strategies, the marks on the right-hand side axis to the different extensions here proposed; the points at the intersections represent the 18 different pipelines tested.

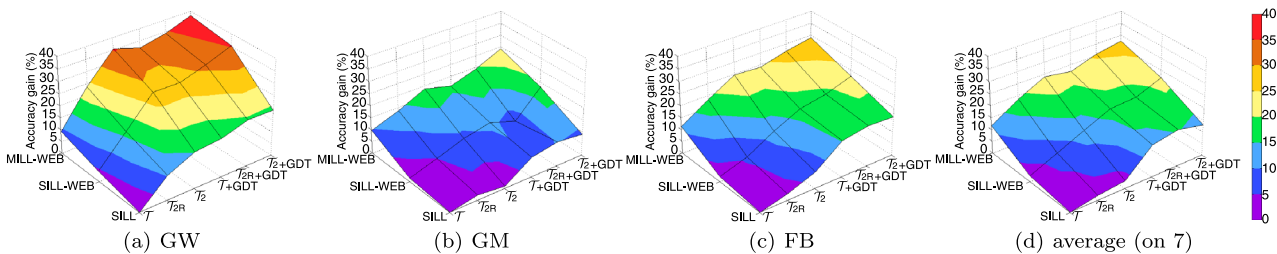


Fig. 2 Percentage improvement of the colorimetric error by the different extended pipelines on the images acquired with the Canon 1D

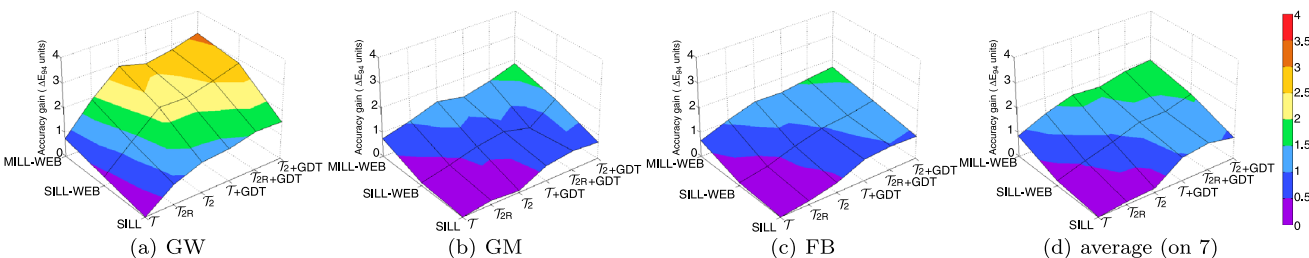


Fig. 3 Absolute improvement of the colorimetric error by the different extended pipelines on the images acquired with the Canon 1D

Table 3 Color correction pipeline accuracy comparison on the images acquired with the Canon 1D

	\mathcal{T} avg. ΔE_{94}	\mathcal{T}_2 avg. ΔE_{94}	\mathcal{T}_{2R} avg. ΔE_{94}	$\mathcal{T} + \text{GDT}$ avg. ΔE_{94}	$\mathcal{T}_2 + \text{GDT}$ avg. ΔE_{94}	$\mathcal{T}_{2R} + \text{GDT}$ avg. ΔE_{94}
SILL ID	4.93	4.71	4.92	4.02	3.97	3.94
SILL GW	8.11	6.88	7.28	6.80	6.57	6.54
SILL WP	10.22	11.35	10.81	8.79	9.86	8.70
SILL SOG	7.41	7.21	7.24	6.64	6.61	6.50
SILL GGW	7.40	7.15	7.21	6.54	6.50	6.40
SILL GM	7.61	7.53	7.44	6.98	6.92	6.83
SILL FB	5.79	5.39	5.63	4.91	4.85	4.81
SILLWEB ID	4.83	4.39	4.71	3.97	3.77	3.86
SILLWEB GW	7.75	5.83	6.79	5.85	5.25	5.58
SILLWEB WP	9.86	10.02	9.43	8.50	8.98	9.03
SILLWEB SOG	7.27	6.47	6.97	6.45	5.89	6.25
SILLWEB GGW	7.26	6.53	6.98	6.32	5.81	6.12
SILLWEB GM	7.50	6.93	7.23	6.75	6.24	7.03
SILLWEB FB	5.67	5.09	5.46	4.80	4.48	4.69
MILLWEB ID	4.07	3.47	3.79	3.69	3.35	3.46
MILLWEB GW	7.37	5.23	6.19	5.51	5.00	5.31
MILLWEB WP	8.44	8.66	8.02	7.80	8.16	7.45
MILLWEB SOG	6.86	5.80	6.37	6.17	5.58	5.95
MILLWEB GGW	6.73	5.79	6.28	6.05	5.58	5.72
MILLWEB GM	6.87	6.18	6.57	6.40	5.77	6.13
MILLWEB FB	5.13	4.36	4.72	4.40	4.11	4.23

Table 4 Color correction pipeline accuracy comparison on the images acquired with the Canon 5D

	\mathcal{T} avg. ΔE_{94}	\mathcal{T}_2 avg. ΔE_{94}	\mathcal{T}_{2R} avg. ΔE_{94}	$\mathcal{T} + \text{GDT}$ avg. ΔE_{94}	$\mathcal{T}_2 + \text{GDT}$ avg. ΔE_{94}	$\mathcal{T}_{2R} + \text{GDT}$ avg. ΔE_{94}
SILL ID	5.18	5.20	4.98	4.74	4.52	4.71
SILL GW	10.21	9.47	10.18	9.54	9.06	9.47
SILL WP	9.48	9.05	9.69	8.88	8.26	8.94
SILL SOG	8.05	7.09	7.95	6.27	5.99	6.30
SILL GGW	7.51	6.99	7.39	6.01	5.73	6.22
SILL GM	6.84	6.58	6.71	5.57	5.68	5.83
SILL FB	6.23	5.88	6.12	4.60	4.57	4.47
SILLWEB ID	4.99	4.31	4.68	3.66	3.83	3.51
SILLWEB GW	8.99	6.56	7.94	6.78	6.32	6.87
SILLWEB WP	9.02	7.82	8.61	8.31	6.99	8.07
SILLWEB SOG	7.66	5.96	7.06	5.93	5.62	5.58
SILLWEB GGW	7.22	5.84	6.71	5.61	5.45	5.34
SILLWEB GM	6.63	5.86	6.28	5.36	5.33	5.12
SILLWEB FB	5.99	5.05	5.63	4.52	4.48	4.33
MILLWEB ID	4.75	3.80	4.38	3.37	3.26	3.03
MILLWEB GW	8.59	6.84	7.60	6.37	6.41	6.58
MILLWEB WP	7.80	6.62	6.80	6.41	6.55	6.23
MILLWEB SOG	7.29	5.19	6.61	5.39	5.02	5.02
MILLWEB GGW	6.90	5.26	6.29	5.14	5.06	4.83
MILLWEB GM	6.32	5.20	5.86	5.12	4.83	4.81
MILLWEB FB	5.72	4.22	5.23	4.20	4.02	3.84

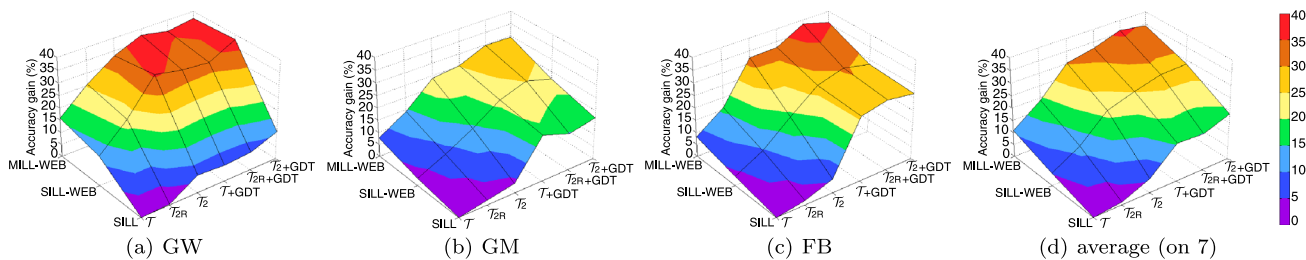


Fig. 4 Percentage improvement of the colorimetric error by the different extended pipelines on the images acquired with the Canon 5D

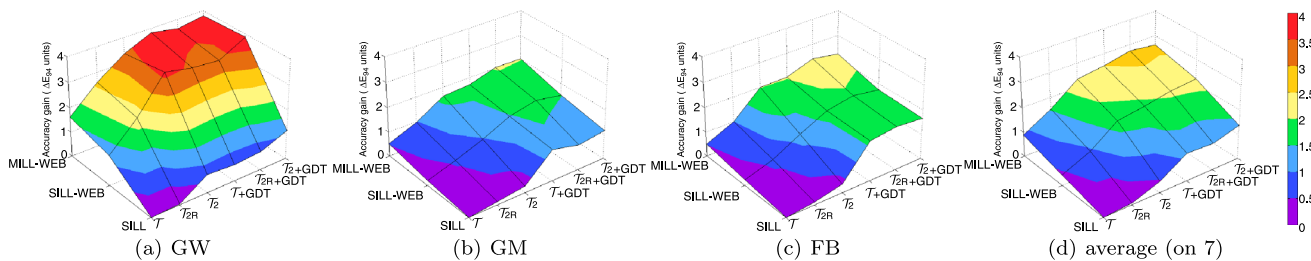


Fig. 5 Absolute improvement of the colorimetric error by the different extended pipelines on the images acquired with the Canon 5D

The points at the intersection of the left axis with the first mark on the right axis, represent the strategies proposed in [12], where 3×3 color correction matrices were used. The ranking on real data of these pipelines proposed in [12] is here confirmed. In particular, the SILL-WEB strategy improves the colorimetric accuracy over the SILL strategy by 3.8 % (0.31 ΔE_{94} units), and the MILL-WEB by 11.2 % (0.87 ΔE_{94} units). Taking the traditional SILL strategy as baseline, the extended SILL strategy improves the results up to 15.7 % (1.13 ΔE_{94} units). It is worth noting that this improvement is larger than that obtained by the original SILL-WEB and MILL-WEB color correction pipelines. Our proposals get better results: the extended SILL-WEB pipeline improves over the baseline up to 25.1 % (1.90 ΔE_{94} units), which is a 21.3 % improvement over the original SILL-WEB; the extended MILL-WEB pipeline improves over the baseline up to 31.0 % (2.31 ΔE_{94} units), which is a 19.75 % improvement over the original MILL-WEB.

A more detailed analysis is given in Figs. 2–5 and Tables 3 and 4 considering separately the two cameras in the dataset and the AWB algorithms considered. The plots are relative to AWB algorithms belonging to three different classes: low-level statistics based (GW), gamut mapping based (GM), and classification based (FB). In the last column, the average gain over the 7 AWB algorithms considered is plotted. In Fig. 3 the absolute colorimetric accuracy gain are plotted. In Fig. 4 and 5 the percentage and absolute colorimetric accuracy gain for the Canon 5D are respectively plotted. The complete numerical values are respective reported in Tables 3 and 4.

It is worth noting that even very simple AWB algorithms like the Gray World, used within the proposed extended

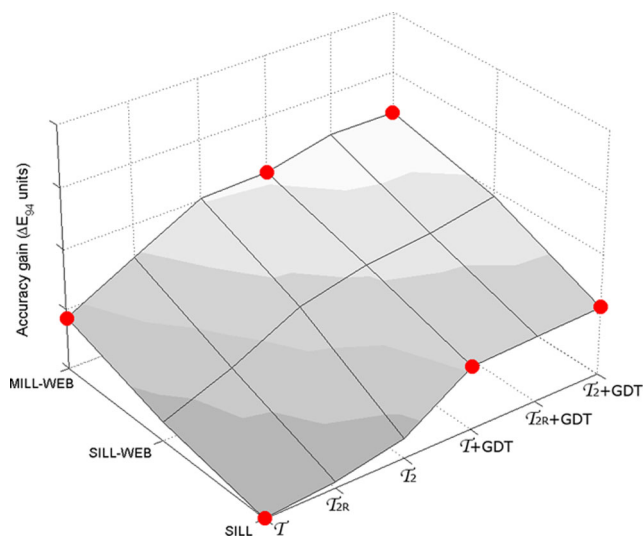


Fig. 6 The red dots identify the different pipelines compared in Fig. 7

pipelines, have similar color rendition accuracy to more complex AWB algorithms requiring a feature extraction and classification stages, used within the traditional pipeline.

An example image is reported in Fig. 7: it belongs to the subset acquired by the Canon 5D and the AWB algorithm used is the GW. The different pipelines compared are reported as red dots in Fig. 6. The average sRGB values of the MCC of each image are extracted and reported in Fig. 8. Each patch is made of two triangles: the upper one represents the ground truth values of the MCC [24], the lower one the values extracted from the image on which the ΔE_{94} colorimetric error between them is overlaid.



Fig. 7 Example image processed with different color correction pipelines

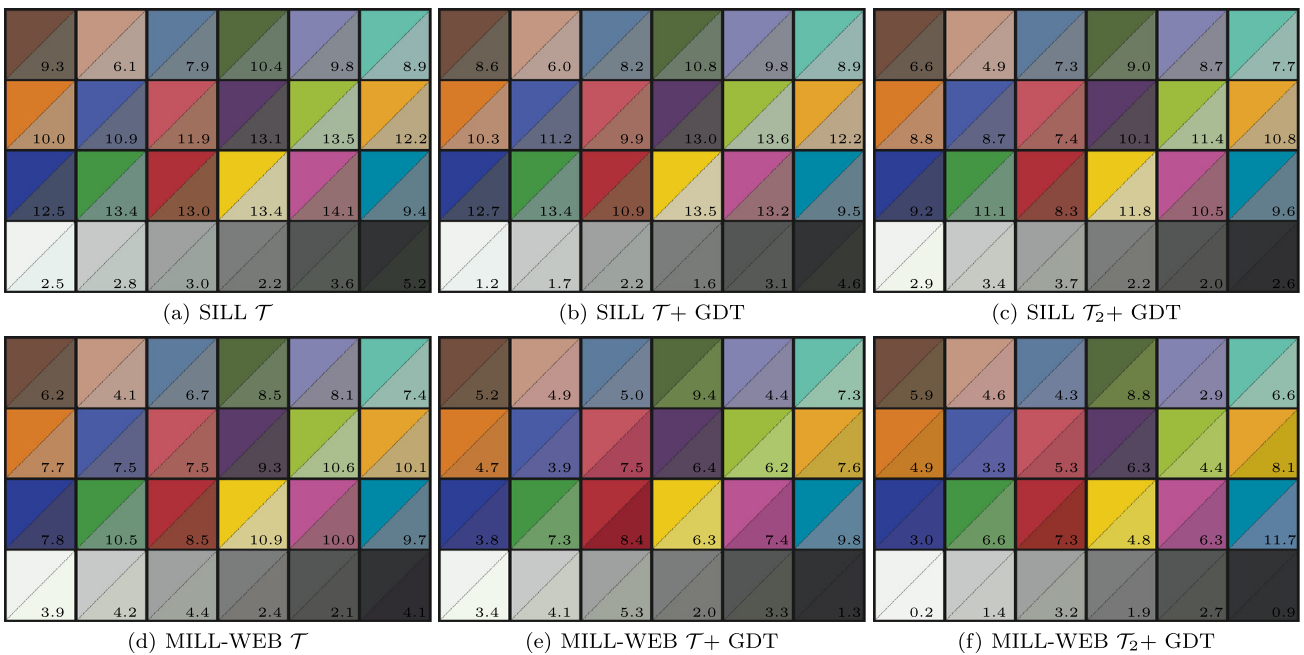


Fig. 8 Comparison between the average sRGB values of the MCC of each image reported in this figure and its ground truth values. Each patch is made of *two triangles*: the upper one represents the ground

truth values of the MCC [24], the lower one the values extracted from the image on which the ΔE_{94} colorimetric error between them is overlaid

5 Conclusion

In this work we have investigated possible extensions of the color correction pipeline for digital photography which exploit the crosstalks between the illuminant estimation and color matrix transformation modules to lead to a higher

color rendition accuracy. The terms of the extended color correction pipelines are found by optimization. Experimental results on a standard dataset of RAW images show the feasibility of the proposed extended pipelines whatever the illuminant estimation algorithm used. Averaging over the different illuminant estimation algorithms tested, the color

correction pipelines proposed in [12] were able to improve the color accuracy with respect to the standard color processing pipeline up to 11.2 %. This improvement can be raised up to 31.0 % using the most performing extended pipeline proposed here.

As a future work, we plan to investigate the applicability of the proposed pipelines to multispectral imaging and to extend the methods to render scenes having multiple illuminants.

References

- Sharma, G.: Digital Color Imaging Handbook. CRC Press, Boca Raton (2002)
- Ramanath, R., Snyder, W.E., Yoo, Y., Drew, M.S.: Color image processing pipeline. *IEEE Signal Process. Mag.* **22**(1), 34–43 (2005)
- Adams, J.E., Hamilton, J.F.: Digital Camera Image Processing Chain Design. Single-Sensor Imaging. CRC Press, Boca Raton (2009)
- Hordley, S.D.: Scene illuminant estimation: past, present, and future. *Color Res. Appl.* **31**(4), 303–314 (2006)
- Ebner, M.: Color Constancy. Wiley, London (2007)
- Foster, D.H.: Color constancy. *Vis. Res.* **51**, 674–700 (2011)
- Gijzen, A., Gevers, T., van de Weijer, J.: Computational color constancy: survey and experiments. *IEEE Trans. Image Process.* **20**(9), 2475–2489 (2011)
- Finlayson, G.D., Drew, M.S.: Constrained least-squares regression in color spaces. *J. Electron. Imaging* **6**, 484–493 (1997)
- Hubel, P.M., Holm, J., Finlayson, G.D., Drew, M.S.: Matrix calculations for digital photography. In: Proceedings of the IS&T/SID 5th Color Imaging Conference, pp. 105–111 (1997)
- Bianco, S., Gasparini, F., Russo, A., Schettini, R.: A new method for RGB to XYZ transformation based on pattern search optimization. *IEEE Trans. Consum. Electron.* **53**(3), 1020–1028 (2007)
- Burns, P.D., Berns, R.S.: Error propagation analysis in color measurement and imaging. *Color Res. Appl.* **22**(4), 280–289 (1997)
- Bianco, S., Bruna, A., Naccari, F., Schettini, R.: Color space transformations for digital photography exploiting information about the illuminant estimation process. *J. Opt. Soc. Am. A* **29**(3), 374–384 (2012)
- von Kries, J.: Chromatic Adaptation. Festschrift der Albrecht-Ludwig-Universität, Fribourg (1902). Translation: MacAdam, D.L.: Sources of color science. MIT Press, Cambridge (1970)
- Finlayson, G.D., Hordley, S.D.: Color by correlation: a simple, unifying framework for color constancy. *IEEE Trans. Pattern Anal. Mach. Intell.* **23**(11), 1209–1221 (2001)
- Bianco, S., Gasparini, F., Schettini, R.: Consensus based framework for illuminant chromaticity estimation. *J. Electron. Imaging* **17**(2), 023013 (2008)
- Finlayson, G.D.: Color constancy in diagonal chromaticity space. In: *IEEE Proc. 5th International Conference on Computer Vision*, pp. 218–223 (1995)
- Van De Weijer, J., Gevers, T., Gijzen, A.: Edge-based color constancy. *IEEE Trans. Image Process.* **16**(9), 2207–2214 (2007)
- Buchsbaum, G.: A spacial processor model for object color perception. *J. Franklin Inst.* **310**, 1–26 (1980)
- Cardei, V., Funt, B., Barnard, K.: White point estimation for uncalibrated images. In: Proceedings of the IS&T/SID 7th Color Imaging Conference, pp. 97–100 (1999)
- Finlayson, G., Trezzi, E.: Shades of gray and colour constancy. In: Proceedings IS&T/SID 12th Color Imaging Conference, pp. 37–41 (2004)
- Bianco, S., Ciocca, G., Cusano, C., Schettini, R.: Improving color constancy using indoor-outdoor image classification. *IEEE Trans. Image Process.* **17**(12), 2381–2392 (2008)
- Bianco, S., Ciocca, G., Cusano, C., Schettini, R.: Automatic color constancy algorithm selection and combination. *Pattern Recognit.* **43**, 695–705 (2010)
- Gehler, P.V., Rother, C., Blake, A., Minka, T., Sharp, T.: Bayesian color constancy revisited. In: Proceedings of the IEEE Computer Society Conference on Computer Vision and Pattern Recognition (CVPR 2008), pp. 1–8 (2008)
- Pascale, D.: RGB coordinates of the Macbeth ColorChecker, pp. 1–16 (2006). <http://www.babelcolor.com/download/>
- Hartigan, J.A., Wong, M.A.: Algorithm AS136: a *k*-means clustering algorithm. *Appl. Stat.* **28**, 100–108 (1979)
- Bianco, S., Schettini, R., Vanneschi, L.: Empirical modeling for colorimetric characterization of digital cameras. In: Proceedings of IEEE International Conference on Image Processing (ICIP'09), pp. 3469–3472 (2009)
- Forsyth, D.A.: A novel algorithm for color constancy. *Int. J. Comput. Vis.* **5**(1), 5–36 (1990)
- Shi, L., Funt, B.V.: Re-processed Version of the Gehler Color Constancy Database of 568 Images. Available online <http://www.cs.sfu.ca/~colour/data/>. Last access: 22 May, 2012
- Finlayson, G.D., Mackiewicz, M., Hurlbert, A.: Root-polynomial colour correction. In: Proceedings of the IS&T/SID 19th Color and Imaging Conference, pp. 115–119 (2011)
- Bianco, S., Gasparini, F., Schettini, R., Vanneschi, L.: Polynomial modeling and optimization for colorimetric characterization of scanners. *J. Electron. Imaging* **17**(4), 043002 (2008)
- Bianco, S., Cusano, C.: Color target localization under varying illumination conditions. In: Computational Color Imaging Workshop 2011. LNCS, vol. 6626, pp. 245–255 (2011)
- Kang, H.R.: Computational Color Technology, vol. PM159. SPIE Press, Bellingham (2006)
- Finlayson, G.D., Drew, M.S., Funt, B.V.: Color constancy: generalized diagonal transforms suffice. *J. Opt. Soc. Am. A* **11**(11), 3011–3019 (1994)
- Bianco, S., Schettini, R.: Computational color constancy. In: 3rd European Workshop of Visual Information Processing (EUVIP), pp. 1–7 (2011)
- Fairchild, M.D.: Color Appearance Models. Addison-Wesley, Reading (1998)
- Bianco, S., Schettini, R.: Two new von Kries based chromatic adaptation transforms found by numerical optimization. *Color Res. Appl.* **35**(3), 184–192 (2010)
- Smoyer, E.P., Taplin, L.A., Berns, R.S.: Experimental evaluation of museum case study digital camera systems. In: Proceedings of the IS&T 2005 Archiving Conference, pp. 85–89 (2005)
- Lewis, R.M., Torczon, V.: Pattern search algorithms for bound constrained minimization. *SIAM J. Control Optim.* **9**, 1082–1099 (1999)
- Lewis, R.M., Torczon, V.: Pattern search methods for linearly constrained minimization. *SIAM J. Control Optim.* **10**, 917–941 (2000)
- Funt, B., Jiang, H.: Nondiagonal color correction. In: Proceedings of the 2003 International Conference on Image Processing (ICIP 2003), pp. 481–484 (2003)
- Land, E.H.: The retinex theory of color vision. *Sci. Am.* **237**(6), 108–128 (1977)
- Ebner, M.: Color constancy based on local space average color. *Mach. Vis. Appl.* **20**(5), 283–301 (2009)
- Bleier, M., Riess, C., Beigpour, S., Eibenberger, E., Angelopoulou, E., Troger, T., Kaup, A.: Color constancy and non-uniform illumination: can existing algorithms work? In: IEEE International Conference on Computer Vision Workshops, pp. 774–781 (2011)

44. Gijssenij, A., Lu, R., Gevers, T.: Color constancy for multiple light sources. *IEEE Trans. Image Process.* **21**(2), 697–707 (2012)
45. Bianco, S., Schettini, R.: Adaptive color constancy using faces. *IEEE Trans. Pattern Anal. Mach. Intell.* (2014). doi:[10.1109/TPAMI.2013.2297710](https://doi.org/10.1109/TPAMI.2013.2297710)



Simone Bianco obtained a Ph.D. in computer science at DISCo (Dipartimento di Informatica, Sistemistica e Comunicazione) of the University of Milano-Bicocca, Italy, in 2010. He obtained B.Sc. and the M.Sc. degrees in mathematics from the University of Milano-Bicocca, Italy, respectively, in 2003 and 2006. He is currently a postdoc working on image processing. The main topics of his current research concern digital still cameras processing pipelines, color space conversions, optimization techniques, and characterization of imaging devices.



Raimondo Schettini is a professor at the University of Milano Bicocca (Italy). He is vice director of the Department of Informatics, Systems and Communication, and head of Imaging and Vision Lab (www.ivl.disco.unimib.it). He has been associated with Italian National Research Council (CNR) since 1987 where he has headed the Color Imaging lab from 1990 to 2002. He has been team leader in several research projects and published more than 250 refereed papers and six patents about color reproduction and image processing, analysis, and classification. He has been recently elected fellow of the International Association of Pattern Recognition (IAPR) for his contributions to pattern recognition research and color image analysis.